

# Multiantenna detection of multicarrier primary signals exploiting spectral *a priori* information

Roberto López-Valcarce, Gonzalo Vazquez-Vilar and Marcos Álvarez-Díaz

Departamento de Teoría de la Señal y las Comunicaciones

Universidad de Vigo, 36310 Vigo, Spain

email: {valcarce, gvazquez, malvarez}@gts.tsc.uvigo.es

**Abstract**—We consider the problem of detecting a primary signal over a wireless channel by a multiantenna cognitive spectral monitor with knowledge of the spectral shape of primary transmissions employing multicarrier modulation. As a starting point, a Locally Most Powerful (LMP) test is derived for the single-antenna case. The asymptotic performance improvement of the LMP detector over the standard Energy Detector (ED) is quantified in terms of the primary spectral mask. For the case of an ideal bandpass mask the LMP test is Uniformly Most Powerful. With multiple antennas, optimal detectors require channel knowledge and therefore are not well suited to practical implementation. We propose a realizable multiantenna Incoherent Detector, and compare its performance with that of the ED and LMP single-antenna tests under both deterministic and Rayleigh slow-fading channel scenarios. In the latter setting, multiple antennas introduce detection diversity that determines the slope of the probability of miss curve, and thus the overall detection performance.

## I. INTRODUCTION

In the last years we have witnessed the paradox of the apparent scarcity of spectral resources while most of the allocated spectrum is underutilized. This fact motivates the concept of spectrum reuse addressed by the Dynamic Spectrum Access / Cognitive Radio paradigm [1]. The key idea of opportunistically accessing temporally and/or spatially unused licensed bands requires powerful spectrum monitoring techniques, since the interference produced to licensed (primary) users must be kept at sufficiently low levels. The nature of wireless channels makes reliable detection of primary users a challenging task: due to fading and shadowing phenomena, the received primary signal may be very weak, resulting in negative Signal-to-Noise Ratio (SNR) operation conditions [2].

Powerful detectors can in principle be derived by exploiting certain properties of the primary signal, such as the presence of any pilots or cyclostationary features. However, these detectors are very sensitive to synchronization errors [2]. With very low SNR, the synchronization loops of the monitoring systems cannot be expected to provide the required accuracy for the frequency and clock rate estimates. On the other hand, the popular energy detector is robust to sync errors, does not require any *a priori* knowledge of primary signals, and has

lower complexity than other sensing schemes. These desirable traits come at the cost of a reduced detection performance [2].

Hence, one may ask whether there are any primary signal features that could be exploited by a detector without requiring accurate synchronization. For example, knowledge of the spectral shape of primary transmissions is usually available to the secondary network. We adopt a weak signal assumption in order to obtain a Locally Most Powerful test resulting in an asynchronous detector which happens to incorporate this kind of information.

Another way to enhance detection power is to exploit the availability of multiple antennas at the secondary terminal. Multiple-input multiple-output (MIMO) technologies have reached maturity and it is very likely that future Cognitive Radio networks will incorporate this type of hardware [3], [4]. As in wireless communication reception, multiple antennas provide spatial diversity when the detector faces fading channels. In [5] a performance analysis was presented for the multiantenna energy detector using maximal ratio combining and antenna selection. These schemes require knowledge of the channel from the primary user to the cognitive node and therefore are difficult to implement in practice.

The detectors considered in this paper, which do not need channel state information, exploit knowledge about some primary network parameters (such as channelization, modulation type, etc.) that may be available to the cognitive node. This information is translated into knowledge about the spectral shape (or equivalently, the autocorrelation) of the primary signal. Spectral shape knowledge is reasonable in many practical cases, in particular for broadcast primary networks. If in addition primary transmitters use multicarrier modulation, then a mathematically tractable Gaussian model can be adopted. Under this assumption we propose and analyze the performance of a practical multiantenna Incoherent Detector (ID) and compare it to both the Energy Detector (ED) and the Locally Most Powerful (LMP) test for the single antenna case, for both deterministic and Rayleigh fading channels.

The rest of this paper is organized as follows. Section II presents the system model. Both the ED and LMP single-antenna detectors are analyzed in Section III, whereas the multiantenna ID test is presented in Section IV. Numerical results and final conclusions are given in Sections V and VI, respectively.

---

This work was supported by the Spanish Government under projects SPROACTIVE (reference TEC2007-68094-C02-01/TCM) and COMONSENS (CONSOLIDER-INGENIO 2010 CSD2008-00010).

## II. SYSTEM MODEL

It is assumed that primary users employ Frequency Division Multiplexing with fixed channelization, known to the spectrum monitor. The cognitive receiver has  $M$  antennas with their respective Radio Frequency (RF) chains. At each antenna, a single primary channel is selected and downconverted to baseband, where it is asynchronously sampled at  $f_s$  samples/s, thus obtaining  $K$  complex-valued samples ( $T = K/f_s$  is the observation time). The samples  $r_k^{(m)}$  at the  $m$ th RF chain are given by

$$r_k^{(m)} = h_m x_k + \sigma w_k^{(m)}, \quad 1 \leq m \leq M, \quad 0 \leq k \leq K-1, \quad (1)$$

where  $x_k$  are the (noiseless) samples of the primary signal, normalized to unit variance ( $E\{|x_k^{(m)}|^2\} = 1$ );  $w_k^{(m)}$  are samples of a zero mean, circular complex white Gaussian noise with unit variance;  $h_m$  is the complex channel gain at antenna  $m$ , and thus  $|h_m|^2$  is the power of the primary signal at that antenna (if the channel is vacant  $|h_m|^2 = 0$  for all  $m$ ); and  $\sigma^2 > 0$  is the background noise power, assumed known and equal at all the antennas. The noise processes at different antennas are assumed independent. We can rewrite (1) as

$$\mathbf{r}_m = h_m \mathbf{x} + \sigma \mathbf{w}_m, \quad 1 \leq m \leq M, \quad (2)$$

with the obvious definitions for the  $K \times 1$  vectors  $\mathbf{r}_m$ ,  $\mathbf{x}$ ,  $\mathbf{w}_m$ . Also, introducing the vectors  $\mathbf{r} \doteq [\mathbf{r}_1^T \mathbf{r}_2^T \cdots \mathbf{r}_M^T]^T$ ,  $\mathbf{w} \doteq [\mathbf{w}_1^T \mathbf{w}_2^T \cdots \mathbf{w}_M^T]^T$ ,  $\mathbf{h} \doteq [h_1 \ h_2 \ \cdots \ h_M]^T$  and denoting the Kronecker product by  $\otimes$ , (2) can be compactly rewritten as

$$\mathbf{r} = \mathbf{h} \otimes \mathbf{x} + \sigma \mathbf{w}. \quad (3)$$

The (asynchronously sampled) process  $\{x_k\}$  can be taken as wide-sense stationary with psd  $S_{xx}(e^{j\omega})$ . In addition, if the primary users employ multicarrier modulation, it is reasonable to assume (for the number of subcarriers used in practical systems) that  $\{x_k\}$  is circular Gaussian. Hence,  $\mathbf{x}$  is zero-mean circular Gaussian with covariance matrix  $\mathbf{C} \doteq E\{\mathbf{x}\mathbf{x}^H\}$ . Assuming that the channelization and modulation parameters of the primary system are fixed and public (as would be the case, e.g. for broadcast networks), then  $S_{xx}(e^{j\omega})$  is known (and so is  $\mathbf{C}$ ). Note that  $\mathbf{C}$  is Toeplitz with ones on the diagonal. In general,  $\{x_k\}$  will be colored (and  $\mathbf{C} \neq \mathbf{I}$ ) as a result of interchannel guard bands, pulse shaping, etc.

Let  $\mathbf{C} = \mathbf{U}\mathbf{\Lambda}\mathbf{U}^H$  with  $\mathbf{\Lambda} = \text{diag}(\lambda_0 \ \lambda_1 \ \cdots \ \lambda_{K-1})$  be an eigendecomposition of  $\mathbf{C}$ . It is well known [6] that for  $K \rightarrow \infty$  (long observation time), then

$$\mathbf{U} \rightarrow \mathbf{W}, \quad \lambda_k \rightarrow S_{xx}(e^{j\frac{2\pi k}{K}}), \quad 0 \leq k \leq K-1, \quad (4)$$

with  $\mathbf{W}$  the  $K \times K$  orthonormal IDFT matrix. In the sequel we will make use of these asymptotic results.

## III. SINGLE ANTENNA DETECTORS

We analyze the detection problem for the single antenna case as starting point. When  $M = 1$ , (3) reduces to

$$\mathbf{r} = h\mathbf{x} + \sigma\mathbf{w}, \quad (5)$$

and the detection problem is summarized as

$$\begin{aligned} \mathcal{H}_0 : \quad & |h|^2 = 0 \quad (\text{primary is absent}) \quad (6) \\ \mathcal{H}_1 : \quad & |h|^2 > 0 \quad (\text{primary is present}) \quad (7) \end{aligned}$$

This hypothesis test is composite since  $|h|^2$  is unknown. Since the test is one-sided, a uniformly most powerful (UMP) test may exist [6]. Note that  $\mathbf{r} \sim \mathcal{CN}(\mathbf{0}, \sigma^2 \mathbf{I})$  under  $\mathcal{H}_0$  and  $\mathbf{r} \sim \mathcal{CN}(\mathbf{0}, |h|^2 \mathbf{C} + \sigma^2 \mathbf{I})$  under  $\mathcal{H}_1$ . The Neyman-Pearson (NP) test for this Gaussian detection problem is an estimator-correlator [6] deciding  $\mathcal{H}_1$  if  $\mathbf{r}^H \hat{\mathbf{x}}$  exceeds a threshold, where

$$\hat{\mathbf{x}} = |h|^2 \mathbf{C} (|h|^2 \mathbf{C} + \sigma^2 \mathbf{I})^{-1} \mathbf{r} \quad (8)$$

is the (scaled) MMSE estimator of  $\mathbf{x}$  (given  $\mathbf{r}$  and  $|h|^2$ ). Unfortunately, the NP test (8) is not implementable in general since it requires knowledge of  $|h|^2$ . However, two limit scenarios are of interest as they result in practical tests:

- High SNR case with a full rank  $\mathbf{C}$ :  $|h|^2 \gg \sigma^2$ , so that  $\hat{\mathbf{x}} \approx \frac{1}{\sigma^2} \mathbf{r}$ . The NP test reduces to an Energy Detector (ED) that decides  $\mathcal{H}_1$  if  $\mathbf{r}^H \mathbf{r}$  exceeds a threshold.
- Low SNR case:  $|h|^2 \ll \sigma^2$  and  $\hat{\mathbf{x}} \approx \frac{|h|^2}{\sigma^4} \mathbf{C} \mathbf{r}$ . The NP test reduces to a *weighted* ED deciding  $\mathcal{H}_1$  if  $\mathbf{r}^H \mathbf{C} \mathbf{r}$  exceeds a threshold. This is the *Locally Most Powerful* (LMP) test, derived from weak signal detection theory [6].

Note that, in contrast to the ED test, the LMP test makes use of the available information about the primary signal spectrum.

Multicarrier signals are well approximated as bandpass processes with a flat passband. For this particular scenario of practical importance, the LMP test becomes UMP as  $K \rightarrow \infty$ . To see this, note that the NP test statistic is

$$\mathbf{r}^H \hat{\mathbf{x}} = \sum_{k=0}^{K-1} \frac{|h|^2 \lambda_k}{|h|^2 \lambda_k + \sigma^2} |v_k|^2, \quad (9)$$

where  $\mathbf{v} \doteq \mathbf{U}^H \mathbf{r} = [v_0 \ v_1 \ \cdots \ v_{K-1}]^T$ . For a bandpass signal,  $S_{xx}(e^{j\omega})$  takes only the values 0 (outside the passband) and  $\lambda > 0$  (inside the passband). Thus, in view of (4), as  $K \rightarrow \infty$ , and with  $\mathcal{B}$  the set of indices corresponding to the passband,

$$\mathbf{r}^H \hat{\mathbf{x}} \rightarrow \sum_{k \in \mathcal{B}} \frac{|h|^2 \lambda}{|h|^2 \lambda + \sigma^2} |v_k|^2 \propto \lambda \sum_{k \in \mathcal{B}} |v_k|^2 = \mathbf{r}^H \mathbf{C} \mathbf{r}, \quad (10)$$

which is the statistic of the LMP test. In contrast to the ED test, which measures the energy in the whole Nyquist bandwidth, the LMP test compares only the energy in the passband to a threshold. This is intuitively satisfying.

### A. Asymptotic Performance of the LPM Test

Let  $T_{\text{LMP}} \doteq \mathbf{r}^H \mathbf{C} \mathbf{r}$ . We can obtain the asymptotic detection performance of the LMP test invoking the central limit theorem: for large  $K$ ,  $T_{\text{LMP}}$  is Gaussian distributed, and

$$\begin{aligned} \mu_{\text{LMP}}(h) &\doteq E\{T_{\text{LMP}}\} = \text{Tr}\{\mathbf{C} E\{\mathbf{r}\mathbf{r}^H\}\} \\ &= \text{Tr}\{\mathbf{C} (|h|^2 \mathbf{C} + \sigma^2 \mathbf{I})\} \\ &= |h|^2 b_2 + \sigma^2 b_1, \end{aligned} \quad (11)$$

where we have introduced the coefficients

$$b_n \doteq \text{Tr}\{\mathbf{C}^n\} = \sum_{k=0}^{K-1} \lambda_k^n, \quad n = 0, 1, 2, \dots \quad (12)$$

(Note that  $b_0 = b_1 = K$ ). The variance of  $T_{\text{LMP}}$  is<sup>1</sup>

$$\begin{aligned} \alpha_{\text{LMP}}^2(h) &\doteq \text{var}\{T_{\text{LMP}}\} = \text{Tr}\{(\mathbf{C}_K E\{\mathbf{r}\mathbf{r}^H\})^2\} \\ &= \text{Tr}\{(|h|^2 \mathbf{C}_K^2 + \sigma^2 \mathbf{C}_K)^2\} \\ &= |h|^4 b_4 + 2|h|^2 \sigma^2 b_3 + \sigma^4 b_2. \end{aligned} \quad (13)$$

Therefore, for large  $K$ , the probability of false alarm  $P_{\text{FA}}$  is

$$P_{\text{FA}} \doteq \text{prob}\{T_{\text{LMP}} > \gamma_{\text{LMP}} | \mathcal{H}_0\} = Q\left(\frac{\gamma_{\text{LMP}} - \mu_{\text{LMP}}(0)}{\alpha_{\text{LMP}}(0)}\right), \quad (14)$$

where  $\gamma_{\text{LMP}}$  is the threshold. Since  $P_{\text{FA}}$  does not depend on  $h$ , we can set the threshold  $\gamma_{\text{LMP}}$  for a given target  $P_{\text{FA}}$  as

$$\gamma_{\text{LMP}} = \alpha_{\text{LMP}}(0)Q^{-1}(P_{\text{FA}}) + \mu_{\text{LMP}}(0). \quad (15)$$

Using (11), (13) and (15), the probability of detection follows:

$$\begin{aligned} P_{\text{D}} &\doteq \text{prob}\{T_{\text{LMP}} > \gamma_{\text{LMP}} | \mathcal{H}_1\} = Q\left(\frac{\gamma_{\text{LMP}} - \mu_{\text{LMP}}(h)}{\alpha_{\text{LMP}}(h)}\right) \\ &= Q\left(\frac{\alpha_{\text{LMP}}(0)}{\alpha_{\text{LMP}}(h)}Q^{-1}(P_{\text{FA}}) - \frac{\mu_{\text{LMP}}(h) - \mu_{\text{LMP}}(0)}{\alpha_{\text{LMP}}(h)}\right) \\ &= Q\left(\frac{Q^{-1}(P_{\text{FA}}) - \sqrt{b_2}\zeta}{\sqrt{1 + 2\frac{b_3}{b_2}\zeta + \frac{b_4}{b_2}\zeta^2}}\right), \end{aligned} \quad (16)$$

where  $\zeta \doteq |h|^2/\sigma^2$  is the SNR. A useful measure of detection performance is the deflection coefficient [6], which for the LMP test is asymptotically given by

$$d_{\text{LMP}}^2 \doteq \frac{(\mu_{\text{LMP}}(h) - \mu_{\text{LMP}}(0))^2}{\alpha_{\text{LMP}}^2(h)} = K \frac{\bar{b}_2^2 \zeta^2}{b_2 + 2\bar{b}_3 \zeta + \bar{b}_4 \zeta^2}, \quad (17)$$

after introducing the normalized coefficients  $\bar{b}_n \doteq b_n/K$ .

### B. Asymptotic Performance of the Energy Detector

Let now  $T_{\text{ED}} \doteq \mathbf{r}^H \mathbf{r}$ . Following steps similar to those in the previous section, it is found that for large  $K$ ,  $T_{\text{ED}}$  is Gaussian distributed with expected value and variance given by

$$\mu_{\text{ED}}(h) \doteq E\{T_{\text{ED}}\} = |h|^2 b_1 + \sigma^2 b_0, \quad (18)$$

$$\alpha_{\text{ED}}^2(h) \doteq \text{var}\{T_{\text{ED}}\} = |h|^4 b_2 + 2|h|^2 \sigma^2 b_1 + \sigma^4 b_0. \quad (19)$$

The threshold  $\gamma_{\text{ED}}$  can be set for a given target  $P_{\text{FA}}$  as

$$\gamma_{\text{ED}} = \alpha_{\text{ED}}(0)Q^{-1}(P_{\text{FA}}) + \mu_{\text{ED}}(0). \quad (20)$$

<sup>1</sup>We make use of the fact that, for zero-mean complex circular Gaussian vectors  $\mathbf{x}$ ,  $\mathbf{y}$  and constant matrices  $\mathbf{A}$ ,  $\mathbf{B}$ , it holds that

$$\begin{aligned} E\{(\mathbf{x}^H \mathbf{A} \mathbf{y})(\mathbf{y}^H \mathbf{B} \mathbf{x})\} &= \text{Tr}[\mathbf{A} \cdot E\{\mathbf{y}\mathbf{x}^H\}] \text{Tr}[\mathbf{B} \cdot E\{\mathbf{x}\mathbf{y}^H\}] \\ &\quad + \text{Tr}[\mathbf{A} E\{\mathbf{y}\mathbf{y}^H\} \mathbf{B} E\{\mathbf{x}\mathbf{x}^H\}]. \end{aligned}$$

Using (18), (19) and (20) the probability of detection follows:

$$P_{\text{D}} \doteq \text{prob}\{T_{\text{ED}} > \gamma_{\text{ED}} | \mathcal{H}_1\} \quad (21)$$

$$= Q\left(\frac{Q^{-1}(P_{\text{FA}}) - \frac{b_1}{\sqrt{b_0}}\zeta}{\sqrt{1 + 2\frac{b_1}{b_0}\zeta + \frac{b_2}{b_0}\zeta^2}}\right). \quad (22)$$

Hence, the corresponding deflection coefficient is

$$d_{\text{ED}}^2 \doteq \frac{(\mu_{\text{ED}}(h) - \mu_{\text{ED}}(0))^2}{\alpha_{\text{ED}}^2(h)} = K \frac{\bar{b}_1^2 \zeta^2}{b_0 + 2\bar{b}_1 \zeta + \bar{b}_2 \zeta^2}. \quad (23)$$

### C. Performance Comparison

It is interesting to compare the asymptotic performance of the LMP and ED tests. Since the detection performance increases as the deflection coefficient increases [6], we focus on the ratio  $d_{\text{LMP}}^2/d_{\text{ED}}^2$  for the same number of samples  $K$ :

$$\frac{d_{\text{LMP}}^2}{d_{\text{ED}}^2} = \frac{\bar{b}_2^2(\bar{b}_0 + 2\bar{b}_1\zeta + \bar{b}_2\zeta^2)}{\bar{b}_1^2(\bar{b}_2 + 2\bar{b}_3\zeta + \bar{b}_4\zeta^2)}. \quad (24)$$

In the low SNR region, this ratio goes to

$$\lim_{\zeta \rightarrow 0} \frac{d_{\text{LMP}}^2}{d_{\text{ED}}^2} = \frac{\bar{b}_2^2 \bar{b}_0}{\bar{b}_1^2 \bar{b}_2} = \bar{b}_2 \quad (\text{since } \bar{b}_0 = \bar{b}_1 = 1). \quad (25)$$

Using Szegő's Theorem [7], one has

$$\begin{aligned} \bar{b}_n &\doteq \lim_{K \rightarrow \infty} \bar{b}_n = \lim_{K \rightarrow \infty} \frac{1}{K} \sum_{k=0}^{K-1} \lambda_k^n \\ &= \frac{1}{2\pi} \int_{-\pi}^{\pi} S_{xx}^n(e^{j\omega}) d\omega. \end{aligned} \quad (26)$$

From the fact that  $\{x_k\}$  has unit variance and the Cauchy-Schwarz inequality, it follows that  $\bar{b}_2 \geq 1$ . Therefore,

$$\lim_{K \rightarrow \infty} \lim_{\zeta \rightarrow 0} \frac{d_{\text{LMP}}^2}{d_{\text{ED}}^2} \geq 1, \quad (27)$$

with equality if and only if  $S_{xx}(e^{j\omega}) = 1$  for  $-\pi \leq \omega \leq \pi$ , that is, for white primary signals. In that case  $\mathbf{C} = \mathbf{I}$  and the LMP test reduces to the energy detector.

Let us return to the ideal frequency flat passband model for the multicarrier primary signal, and let  $\bar{B} < 1$  be the fraction of the Nyquist bandwidth occupied by the signal. From (26),

$$\bar{b}_n = \lim_{K \rightarrow \infty} \bar{b}_n = \frac{1}{\bar{B}^{n-1}}, \quad (28)$$

and therefore, for this particular case,

$$\lim_{K \rightarrow \infty} \lim_{\zeta \rightarrow 0} \frac{d_{\text{LMP}}^2}{d_{\text{ED}}^2} = \frac{1}{\bar{B}} > 1, \quad (29)$$

that is, the advantage of the LMP test over the ED test increases as the primary signal becomes more narrowband.

Regarding computational load, the ED test just requires  $K$  complex multiplications and  $K-1$  additions to compute  $\mathbf{r}^H \mathbf{r}$ , and thus its complexity is  $\mathcal{O}(K)$ . For the LMP test, the statistic  $\mathbf{r}^H \mathbf{C} \mathbf{r}$  can be most efficiently computed by obtaining the FFT of the vector  $\mathbf{r}$  and using the asymptotic results (4), resulting in  $\mathcal{O}(K \log K)$  complexity.

#### IV. MULTIPLE ANTENNA DETECTORS

With  $M > 1$  antennas, the received  $MK \times 1$  vector  $\mathbf{r}$  is given by (3), and the corresponding hypothesis test is

$$\mathcal{H}_0 : \quad \|\mathbf{h}\|^2 = 0 \quad (\text{primary is absent}) \quad (30)$$

$$\mathcal{H}_1 : \quad \|\mathbf{h}\|^2 > 0 \quad (\text{primary is present}) \quad (31)$$

which is again composite since  $\mathbf{h}$  is unknown. Now  $\mathbf{r} \sim \mathcal{CN}(\mathbf{0}, \sigma^2 \mathbf{I})$  under  $\mathcal{H}_0$  and  $\mathbf{r} \sim \mathcal{CN}(\mathbf{0}, (\mathbf{h}\mathbf{h}^H \otimes \mathbf{C}) + \sigma^2 \mathbf{I})$  under  $\mathcal{H}_1$ . The NP test decides  $\mathcal{H}_1$  if  $\mathbf{r}^H \hat{\mathbf{x}}$  exceeds a threshold, where now

$$\hat{\mathbf{x}} = (\mathbf{h}\mathbf{h}^H \otimes \mathbf{C}) [(\mathbf{h}\mathbf{h}^H \otimes \mathbf{C}) + \sigma^2 \mathbf{I}]^{-1} \mathbf{r}. \quad (32)$$

In contrast with the single antenna case, neither in the high nor low SNR regimes does the NP test reduce to a test not depending on  $\mathbf{h}$ . For example, for asymptotically small SNR, the statistic of the NP test becomes

$$\mathbf{r}^H \hat{\mathbf{x}} \propto \mathbf{r}^H (\mathbf{h}\mathbf{h}^H \otimes \mathbf{C}) \mathbf{r} = \sum_{i=1}^M \sum_{j=1}^M h_i h_j^* \mathbf{r}_i^H \mathbf{C} \mathbf{r}_j. \quad (33)$$

The main difficulty stems from the fact that, although the parameter defining the hypotheses is  $\|\mathbf{h}\|^2$ , the distribution of  $\mathbf{r}$  under  $\mathcal{H}_1$  depends on all products of the form  $h_i h_j^*$ .

##### A. Multiantenna Incoherent Detector (ID)

One possible detector in this case can be obtained by neglecting the ‘‘off-diagonal terms’’ (i.e.  $i \neq j$ ) in (33) as well as the weights  $|h_i|^2$  in the ‘‘diagonal terms’’ ( $i = j$ ). The resulting test decides  $\mathcal{H}_1$  if

$$T_{\text{ID}} \doteq \sum_{i=1}^M \mathbf{r}_i^H \mathbf{C} \mathbf{r}_i > \gamma_{\text{ID}}, \quad (34)$$

or, upon defining  $\mathbf{Q} \doteq \mathbf{I}_M \otimes \mathbf{C}$ ,

$$T_{\text{ID}} \doteq \mathbf{r}^H \mathbf{Q} \mathbf{r} > \gamma_{\text{ID}}. \quad (35)$$

We refer to (34) as *Incoherent Detection* (ID) test, since it ignores the correlation among different antennas. Note that this detector does not require knowledge of the channel  $\mathbf{h}$ .

The statistic of the multiantenna ID test is the sum of the LMP statistics for each individual antenna. For large  $K$ , we rely again on the central limit theorem to obtain the asymptotic detection performance. The expected value of  $T_{\text{ID}}$  is just

$$\mu_{\text{ID}}(\mathbf{h}) \doteq E\{T_{\text{ID}}\} = \|\mathbf{h}\|^2 b_2 + M\sigma^2 b_1, \quad (36)$$

whereas its variance is given by

$$\begin{aligned} \alpha_{\text{ID}}^2(\mathbf{h}) &\doteq \text{var}\{T_{\text{ID}}\} = \text{Tr}\{(\mathbf{Q}E\{\mathbf{r}\mathbf{r}^H\})^2\} \\ &= \text{Tr}\{(\mathbf{h}\mathbf{h}^H \otimes \mathbf{C}^2 + \sigma^2 \mathbf{I}_M \otimes \mathbf{C})^2\} \\ &= \text{Tr}\{\|\mathbf{h}\|^2 \mathbf{h}\mathbf{h}^H \otimes \mathbf{C}^4 \\ &\quad + 2\sigma^2 \mathbf{h}\mathbf{h}^H \otimes \mathbf{C}^3 + \sigma^4 \mathbf{I}_M \otimes \mathbf{C}^2\} \\ &= \|\mathbf{h}\|^4 b_4 + 2\|\mathbf{h}\|^2 \sigma^2 b_3 + M\sigma^4 b_2 \end{aligned} \quad (37)$$

Therefore, the threshold for a target  $P_{\text{FA}}$  is

$$\gamma_{\text{ID}} = \alpha_{\text{ID}}(\mathbf{0})Q^{-1}(P_{\text{FA}}) + \mu_{\text{ID}}(\mathbf{0}). \quad (38)$$

Using (36), (37) and (38) the probability of detection is found to be

$$\begin{aligned} P_{\text{D}} &\doteq \text{prob}\{T_{\text{ID}} > \gamma_{\text{ID}} \mid \mathcal{H}_1\} = Q\left(\frac{\gamma_{\text{ID}} - \mu_{\text{ID}}(\mathbf{h})}{\alpha_{\text{ID}}(\mathbf{h})}\right) \\ &= Q\left(\frac{\alpha_{\text{ID}}(\mathbf{0})Q^{-1}(P_{\text{FA}}) - \mu_{\text{ID}}(\mathbf{h}) + \mu_{\text{ID}}(\mathbf{0})}{\alpha_{\text{ID}}(\mathbf{h})}\right) \\ &= Q\left(\frac{Q^{-1}(P_{\text{FA}}) - \sqrt{M\bar{b}_2\zeta}}{\sqrt{1 + 2\frac{\bar{b}_3}{\bar{b}_2}\zeta + M\frac{\bar{b}_4}{\bar{b}_2}\zeta^2}}\right) \end{aligned} \quad (39)$$

where  $\zeta$  is now defined as the average SNR per antenna:

$$\zeta \doteq \frac{\|\mathbf{h}\|^2}{M\sigma^2}. \quad (40)$$

The corresponding deflection coefficient is

$$d_{\text{ID}}^2 = KM \frac{\bar{b}_2^2 \zeta^2}{\bar{b}_2 + 2\bar{b}_3 \zeta + M\bar{b}_4 \zeta^2}. \quad (41)$$

##### B. Performance comparison

It is of interest to compare the asymptotic performances of the single-antenna LMP test with  $K$  input samples and the  $M$ -antenna ID test with  $\tilde{K}$  samples per antenna (thus a total of  $\tilde{K}M$  samples), for the same average SNR  $\zeta$ . If  $K \neq \tilde{K}$ , the parameters  $\bar{b}_n$  featuring in (17) are different from those in (41). However, asymptotically as both  $K, \tilde{K} \rightarrow \infty$  they reach the same values  $\bar{b}_n$  in (26), which depend only on the signal psd. Taking this into account, the asymptotic deflection coefficient ratio can be written as

$$\frac{d_{\text{LMP}}^2}{d_{\text{ID}}^2} = \frac{K}{\tilde{K}M} \frac{\bar{b}_2 + 2\tilde{b}_3\zeta + M\tilde{b}_4\zeta^2}{\bar{b}_2 + 2\bar{b}_3\zeta + \bar{b}_4\zeta^2} \quad \text{as } K, \tilde{K} \rightarrow \infty. \quad (42)$$

Hence, in the low SNR regime, one has

$$\lim_{\zeta \rightarrow 0} \frac{d_{\text{LMP}}^2}{d_{\text{ID}}^2} = \frac{K}{\tilde{K}M} \quad \text{as } K, \tilde{K} \rightarrow \infty. \quad (43)$$

On the other hand, the single-antenna LMP test requires one FFT of size  $K$ , whereas the multiple-antenna ID test requires  $M$  FFTs of size  $\tilde{K}$ . The integration times of these detectors are proportional to  $K$  and  $\tilde{K}$  respectively. All these considerations allow different tradeoffs in terms of detection power, computational complexity, and dwelling time (this last quantity is important in cognitive radio systems, since they must scan a large number of primary channels):

- If both single- and multiple-antenna tests process the *same total number of samples*, i.e.  $K = \tilde{K}M$ , then (43) equals 1: both systems achieve the same asymptotic detection performance. Their complexities are  $\mathcal{O}(K \log K)$  and  $\mathcal{O}(K \log \frac{K}{M})$  respectively, favoring the multiantenna scheme, which in addition requires a dwelling time  $M$  times smaller for the same detection power.
- If both systems operate with *equal dwelling times*, i.e.  $K = \tilde{K}$ , then the deflection coefficient is  $M$  times larger for the multiantenna ID test (which now processes  $M$  times more samples than the single-antenna LMP test). The complexities are now  $\mathcal{O}(K \log K)$  and  $\mathcal{O}(MK \log K)$ ; thus, the performance improvement comes with an  $M$ -fold increase in computational load.

### C. Detection Diversity Gain

In the previous sections a deterministic channel has been implicitly assumed. Now we consider a slow fading setting where the channel coefficients are assumed constant over the detector integration time. We model the channel coefficients as Rayleigh distributed with a given correlation matrix  $\Upsilon$  (with  $\text{rank}\{\Upsilon\} = \tilde{M} \leq M$ ) among the multiple antennas:

$$\mathbf{h} \sim \mathcal{CN}(\mathbf{0}, \Upsilon). \quad (44)$$

From (39), the probability of miss is given by

$$P_{\text{Miss}} \doteq 1 - P_{\text{D}} = Q \left( \frac{\sqrt{Mb_2}\zeta - Q^{-1}(P_{\text{FA}})}{\sqrt{1 + 2\frac{b_3}{b_2}\zeta + M\frac{b_4}{b_2}\zeta^2}} \right). \quad (45)$$

Using a first-order Taylor approximation of the argument of the  $Q$ -function in (45) about  $\zeta = 0$ , one finds that in the low SNR regime,

$$P_{\text{Miss}} \approx Q \left[ \left( \sqrt{Mb_2} + \frac{b_3}{b_2} Q^{-1}(P_{\text{FA}}) \right) \zeta - Q^{-1}(P_{\text{FA}}) \right]. \quad (46)$$

In a fading environment,  $P_{\text{Miss}}$  in (46) becomes a random variable. Its mean value can be upper bounded by noting that

$$Q(x) \leq \frac{1}{2} e^{-x/2}, \quad x \geq 0. \quad (47)$$

By using this bound in (46) and then averaging over  $\mathbf{h}$ ,

$$E[P_{\text{Miss}}] \leq \frac{1}{2} \exp \left\{ \frac{Q^{-1}(P_{\text{FA}})}{2} \right\} \times E \left[ \exp \left\{ -\frac{\zeta}{2} \left( \sqrt{Mb_2} + \frac{b_3}{b_2} Q^{-1}(P_{\text{FA}}) \right) \right\} \right] \quad (48)$$

Using similar steps to those in [8, Sec. 4.4], one finds that

$$E[P_{\text{MD}}] \leq C \bar{\zeta}^{-\tilde{M}} \prod_{m=1}^{\tilde{M}} \frac{1}{\epsilon_m} \sum_{k=1}^{\tilde{M}} \epsilon_k, \quad (49)$$

where  $\epsilon_1, \dots, \epsilon_{\tilde{M}}$  are the  $\tilde{M}$  nonzero eigenvalues of  $\Upsilon$ ,

$$\bar{\zeta} \doteq \frac{1}{M\sigma^2} \text{Tr}\{\Upsilon\} \quad (50)$$

is the SNR, and

$$C = \frac{1}{2} \exp \left\{ \frac{Q^{-1}(P_{\text{FA}})}{2} \right\} \left( \frac{2}{\sqrt{Mb_2} + \frac{b_3}{b_2} Q^{-1}(P_{\text{FA}})} \right)^{\tilde{M}} \quad (51)$$

is a constant independent of the SNR and  $\epsilon_1, \dots, \epsilon_{\tilde{M}}$ . Hence the *diversity order*, that is, the slope of  $E[P_{\text{Miss}}]$  versus the SNR when plotted on a log-log scale, is given by the rank of the fading correlation matrix. This shows the advantage of having multiple antennas for channel sensing under fading conditions.

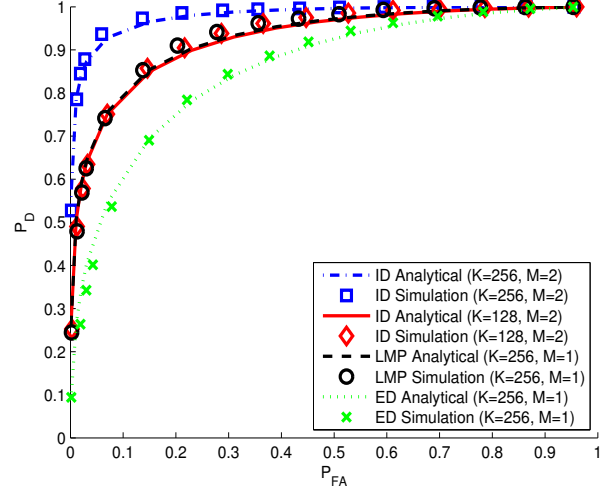


Fig. 1. Receiver Operation Characteristic for the different detectors in a deterministic channel with  $\text{SNR} = -10$  dB.

## V. NUMERICAL RESULTS

The performance of the proposed detectors is tested via Monte Carlo simulations, using a DVB-T reference signal<sup>2</sup> with bandwidth  $B = 7.61$  MHz quantized to 9-bit precision. This channel was downshifted to baseband and asynchronously sampled at  $f_s = 16$  MHz, thus in this case the occupied bandwidth fraction is  $\bar{B} = 0.4756$ . The autocorrelation estimate of this reference signal was used to generate the covariance matrix  $\mathbf{C}$  used by the LMP and ID tests.

### A. Deterministic channels

A low SNR scenario is considered in which the signal is corrupted by white noise with known power. We analyze the performance of the proposed detectors in four different configurations:

- 1) Energy Detector ( $M = 1, K = 256$ )
- 2) Locally Most Powerful Test ( $M = 1, K = 256$ )
- 3) Multiantenna Incoherent Detector ( $M = 2, \tilde{K} = 128$ )
- 4) Multiantenna Incoherent Detector ( $M = 2, \tilde{K} = 256$ )

Fig. 1 shows the  $P_{\text{D}}$  vs.  $P_{\text{FA}}$  tradeoff for  $\text{SNR} = -10$  dB. The results match the asymptotic analysis even for these moderated values of  $K$ . Regarding the performance of the tests, the improvement obtained by exploiting the available knowledge about the signal psd is apparent. It is also seen that the performances of the single-antenna LMP test and the two-antenna ID test when both process the same total number of samples is very similar, as foreseen in Section IV-A, whereas for the same dwelling time, the two-antenna system shows a significant improvement.

In Fig. 2 the probability of miss is plotted in the range  $\text{SNR} \in [-15, -5]$  dB, and for  $P_{\text{FA}} = 0.01$ . For the same total number of samples both the single-antenna LMP and the multiantenna ID tests perform about 3 dB better than the

<sup>2</sup>8K mode, 64-QAM, guard interval 1/4, inner code rate 2/3.

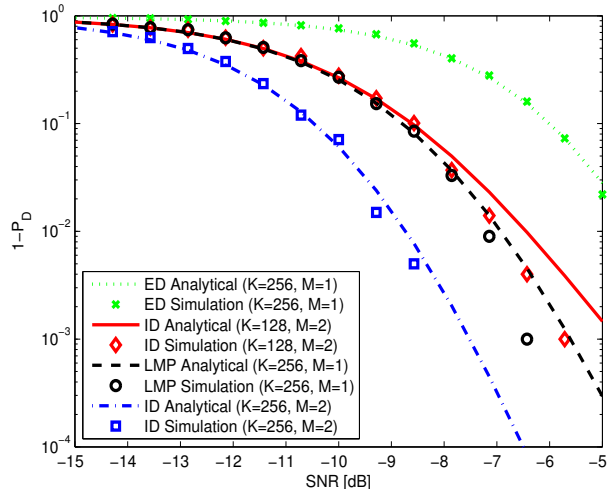


Fig. 2. Detection performance of the different tests as a function of the SNR for fixed  $P_{FA} = 0.01$ .

Energy Detector in the region of interest. If we match the dwelling times of the LMP and ID tests, then the latter offers an additional 2.5 dB gain due to the increased total number of samples. As  $P_D \rightarrow 1$ , simulation results begin to disagree with the analytical curves: these were obtained with an asymptotic probability distribution for large values of  $K$ , and the accuracy of the approximation degrades in this region.

### B. Rayleigh fading channels

We assume independent Rayleigh fading at the multiple antennas. The channel coefficients are drawn from a Gaussian distribution:

$$\mathbf{h} \sim \mathcal{CN}(\mathbf{0}, \rho^2 \mathbf{I}), \quad (52)$$

so that the SNR is  $\bar{\zeta} = \rho^2 / \sigma^2$ . We consider three of the proposed detectors with the same total number of samples, as follows:

- 1) Energy Detector ( $M = 1, K = 512$ ).
- 2) Locally Most Powerful Test ( $M = 1, K = 512$ ).
- 3) Multiantenna Incoherent Detector ( $M = 4, \tilde{K} = 128$ ).

In Fig. 3 the probability of miss has been plotted in the range  $\bar{\zeta} \in [-15, 0]$  dB for  $P_{FA} = 0.01$ . It is seen that the two single-antenna detectors have the same asymptotic slope, whereas ID with 4 antennas has an increased diversity gain that translates in a faster decay for the probability of miss. Note that the asymptotic bound presents in all the cases the right slope, though it becomes looser as the number of antennas increases.

## VI. CONCLUSIONS

In cognitive radio systems it is reasonable to assume that some knowledge about the primary network, such as channelization and modulation type, is available to the secondary users. This information, translated into knowledge of the spectral shape of primary signals, can be exploited in order to enhance signal detection algorithms such as the popular

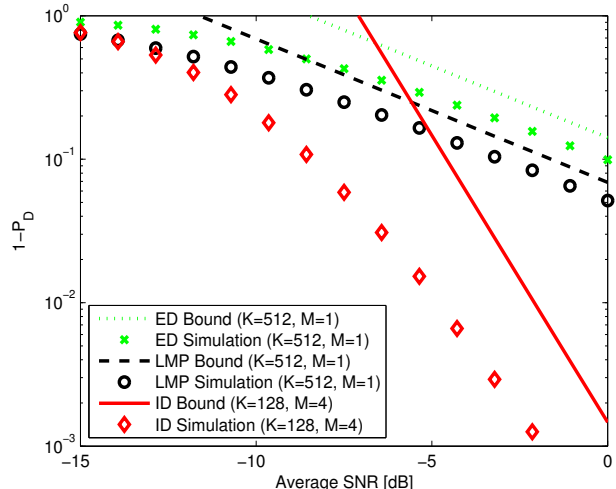


Fig. 3. Detection performance of the different tests in a fading channel as a function of the average SNR for fixed  $P_{FA} = 0.01$ .

Energy Detector. We have presented a single-antenna Locally Most Powerful detector for multicarrier signals, which asymptotically becomes Uniformly Most Powerful if the signal psd is approximated as an ideal bandpass function.

When the spectrum monitor is equipped with multiple antennas, it is not possible to remove the dependence of the optimal Neyman-Pearson detector with the channel coefficients by letting the SNR approach zero. Nevertheless, a suboptimal multiantenna Incoherent Detector has been proposed, which does not need channel knowledge. It can reduce the dwelling time of the single-antenna LMP test maintaining the same detection power, and moreover, for slow fading scenarios it offers a diversity gain in terms of the rate at which the average probability of detection goes to one with increasing SNR. Work is in progress in order to improve on the performance of the Incoherent Detector by exploiting signal correlation among different antennas.

## REFERENCES

- [1] Q. Zhao and B. M. Sadler, "A survey of dynamic spectrum access," *IEEE Signal Processing Mag.*, vol. 24, no. 3, pp. 79–89, May 2007.
- [2] D. Cabric, "Addressing the feasibility of cognitive radios," *IEEE Signal Processing Mag.*, vol. 25, no. 6, pp. 85–93, Nov. 2008.
- [3] R. Zhang and Y.-C. Liang, "Exploiting multi-antennas for opportunistic spectrum sharing in cognitive radio networks," *IEEE J. Sel. Topics Signal Process.*, vol. 2, no. 1, pp. 88–102, Feb. 2008.
- [4] G. Scutari, D. P. Palomar, and S. Barbarossa, "Cognitive MIMO radio," *IEEE Signal Processing Mag.*, vol. 25, no. 6, pp. 46–59, Nov. 2008.
- [5] A. Pandharipande and J.-P. Linnartz, "Performance analysis of primary user detection in a multiple antenna cognitive radio," *Proc. IEEE Int. Conf. Communications (ICC)*, pp. 6482–6486, June 2007.
- [6] S. M. Kay, *Fundamentals of statistical signal processing: detection theory*. Englewood Cliffs, NJ: Prentice-Hall, 1998.
- [7] U. Grenander and G. Szegő, *Toeplitz Forms and Their Applications*. New York: Chelsea: American Mathematical Society, 1984.
- [8] E. G. Larsson and P. Stoica, *Space-Time Block Coding for Wireless Communications*. Cambridge University Press, 2003.